

DEVELOPMENT OF NONDESTRUCTIVE EVALUATION METHODS FOR CERAMIC COATINGS AND MEMBRANES

J. G. Sun

Argonne National Laboratory, Nuclear Engineering Division
9700 S. Cass Ave., Argonne, IL 60439

E-mail: sun@anl.gov; Telephone (630)252-5169; FAX (630)252-2785

ABSTRACT

Nondestructive evaluation (NDE) methods are being developed for thermal barrier coatings (TBCs) and for gas-separation membranes. For TBC applications, current NDE development is focused on infrared thermal imaging methods. Compared with optical and other methods, thermal imaging is quantitative so can be used to characterize TBCs during their entire life cycle, from as-processed condition to service degradation and eventual delamination/spallation. Two thermal imaging methods are being developed: multilayer thermal modeling and thermal tomography. The multilayer-modeling method may determine the thermal property distribution and the thermal tomography method can image the TBC structure in 3D. Recent development in experimental procedure and data processing algorithms has allowed for measurement of TBC thermal conductivity with accuracies comparable to the standard laser flash method. Thermal conductivity is the most important TBC thermophysical property and exhibits characteristic changes during service lifetime. A conductivity-based model to monitor TBC degradation has been proposed. For membrane application, synchrotron x-ray microCT technology was investigated for potential identification of membrane parameters and structural defects based on constructed 3D microstructure data. This paper describes recent developments and experimental results to demonstrate the potential application of these NDE methods.

INTRODUCTION

Advanced structural and functional ceramics have been developed for fossil energy applications to improve efficiency and reduce emission. These include thermal barrier coatings (TBCs) applied on turbine engine components and high-temperature gas-separation membranes. As the materials are improved and their applications are extended, it becomes necessary to establish new characterization methods capable to examine the fundamental material properties and their degradation during service. The present research is focused on developing nondestructive evaluation (NDE) methods for TBCs and ceramic membranes.

Work at Argonne National Laboratory (ANL) is underway to develop quantitative NDE methods for TBCs and membranes. TBCs, applied by electron beam-physical vapor deposition (EB-PVD) or air plasma spraying (APS), allow for metallic components to be utilized at higher temperatures in the hot-gas path of gas turbines, including syngas fired turbines.¹⁻³ TBC failure normally starts from initiation of small cracks at the TBC/bond coat interface. These cracks then grow and link together to form delaminations which eventually cause TBC spallation. TBC thermal properties are important in this degradation process because they determine the thermal gradient that affects stress distribution in crack development. Recent effort at ANL was focused on optical⁴ and thermal-imaging⁵⁻⁷ methods to measure TBC thickness and thermal conductivity. Optical methods are effective for relatively thin TBCs because of limited optical penetration depth. Thermal-imaging methods, on the other hand, are applicable for both thin and thick

TBCs. Two thermal imaging methods are being developed at ANL: multilayer thermal modeling⁵⁻⁶ and thermal tomography⁷. The multilayer-modeling method may determine thermal property distribution of the TBC layer over an entire component surface, and the thermal tomography method can image the TBC depth distributions. The thermal property data may be used to assess TBC degradation condition.

For ceramic membranes that are being developed for hydrogen or oxygen separation, NDE methods can be useful in verifying the dimension distributions and presence of flaws in the materials (leaks). The material systems being examined are dense ceramic membranes deposited on porous ceramic substrates. Synchrotron x-ray microCT (computed tomography) technology was investigated for characterization of membrane structures and defects based on constructed 3D microstructure data. These measurements were performed at the Advanced Photon Source (APS) of ANL.

This paper presents the recent developments for and experimental results from these NDE methods and discusses their applications for material property characterization and material degradation prediction.

THERMAL IMAGING CHARACTERIZATION FOR TBCs

Thermal imaging is based on monitoring the temperature decay on a specimen surface after it is applied with a pulsed thermal energy that is gradually transferred inside the specimen. A schematic one-sided pulsed-thermal-imaging setup for testing a 3-layer material system is illustrated in Fig. 1. The premise is that the heat transfer from the surface (or surface temperature/time response) is affected by internal material structures and properties and the presence of flaws such as cracks^{8,9}.

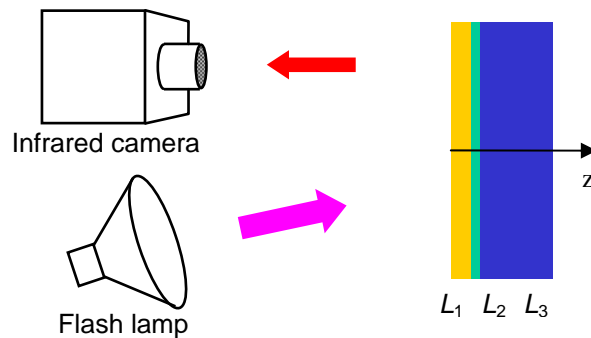


Fig. 1. Schematics of pulsed thermal imaging of a 3-layer material system.

The important TBC parameters to be determined by thermal imaging include the thickness, thermal conductivity and heat capacity (the product of density and specific heat) of the top ceramic TBC layer. These three TBC parameters, however, may not be independent to allow for individual determination from thermal imaging test. To address this issue that is essential for the developed of the multilayer thermal-modeling method, a theoretical analysis was conducted.

Theoretical Analysis of a Two-Layer TBC System

To analyze the surface temperature variation during pulsed thermal imaging, theoretical formulations of the heat transfer process need to be examined. The 1D governing equation for heat conduction in a solid material is:

$$\rho c \frac{\partial T}{\partial t} = \frac{\partial}{\partial z} \left(k \frac{\partial T}{\partial z} \right), \quad (1)$$

where $T(z, t)$ is temperature, ρ is density, c is specific heat, k is thermal conductivity, t is time, z is coordinate in the depth direction, and $z = 0$ is the surface that receives pulsed heating at $t = 0$. It is noted that Eq. (1) contains two independent thermal parameters, the heat capacity ρc and the thermal conductivity k , both are normally assumed constant in each material layer. These two thermal parameters can be converted to another two parameters, the thermal effusivity e ($= (k\rho c)^{1/2}$) and the thermal diffusivity α ($= k/\rho c$). It can be shown that any two of these four thermal parameters are independent and can be used to derive the other two parameters.

Equation (1) indicates that there are three independent TBC parameters: thickness L , thermal conductivity k , and heat capacity ρc . Under ideal flash thermal imaging conditions, i.e., instantaneous flash heating, no volume heat absorption and no heat loss, theoretical solution of the surface temperature for a two-layer material system without interface resistance is¹⁰:

$$T(t) = T_\infty \left[1 + 2 \frac{x_1 \omega_1 + x_2 \omega_2}{x_1 + x_2} \sum_{k=1}^{\infty} \frac{x_1 \cos(\omega_1 \gamma_k) + x_2 \cos(\omega_2 \gamma_k)}{x_1 \omega_1 \cos(\omega_1 \gamma_k) + x_2 \omega_2 \cos(\omega_2 \gamma_k)} \exp\left(-\frac{\gamma_k^2 t}{\eta_2^2}\right) \right], \quad (2)$$

where substrates 1 and 2 are for layers 1 and 2, respectively, γ_k is the K -th positive root of the following equation,

$$x_1 \sin(\omega_1 \gamma) + x_2 \sin(\omega_2 \gamma) = 0, \quad (3)$$

x and ω are defined as,

$$x_i = e_{i2} - (-1)^i, \quad e_i = \sqrt{k_i \rho_i c_i}, \quad i = 1, 2 \quad (4)$$

$$\omega_i = \eta_{i2} - (-1)^i, \quad \eta_i = L_i / \sqrt{\alpha_i}, \quad i = 1, 2 \quad (5)$$

with

$$e_{i2} = e_1 / e_2, \quad \eta_{i2} = \eta_1 / \eta_2. \quad (6)$$

From Eqs. (2)-(6), it is evident that the surface temperature response under flash thermal imaging is controlled by only two parameters (in each layer): the thermal effusivity e and the parameter $\eta = L/\alpha^{1/2}$. This conclusion is significant for thermal imaging analysis of TBCs; it shows that, among the three important TBC parameters L , k and ρc , only two can be determined independently by pulsed thermal imaging¹¹.

TBC Thermal Property Measurement Using Multilayer Thermal Modeling Method

The theoretical solution Eq. (2) cannot be directly used to analyze thermal imaging data because a large number of eigenfunctions in Eq. (3) needs to be calculated and a TBC system may have to be modeled by more than 2 layers. To facilitate thermal imaging analysis of multilayer materials, a multilayer thermal modeling method was developed to solve the heat transfer equation (1) numerically under pulsed thermal imaging condition⁷. In this method, a

TBC is modeled by a multilayer material system and the 1D heat-transfer equation describing the pulsed thermal-imaging process is solved by numerical simulation. The numerical formulation may also incorporate finite heat absorption depth effect due to the TBC translucency and the finite flash duration effect. The numerical solutions (of surface temperature decay) are then fitted with the experimental data at each pixel by least-square minimization to determine unknown parameters in the multilayer material system. Multiple parameters in one or several layers can be determined simultaneously. Among the three parameters for opaque TBCs, the TBC thickness, thermal conductivity and heat capacity, the multilayer modeling method can be configured to calculate two of these three parameters by setting the remaining one at constant. This data fitting process is automated for all pixels within the thermal images and the final results are presented as images of the predicted TBC parameters.

The multilayer modeling method was used to measure TBC thermal properties, conductivity and heat capacity, with known TBC thickness. The experimental sample is an as-processed EBPVD TBC specimen with a surface area of 25.4 mm in diameter (sample courtesy of Dr. A. Feuerstein, Praxair Surface Technologies, Inc.). The top ceramic coating is 0.127 mm thick, and the nickel-based superalloy substrate has a thickness of 3.1 mm. The TBC surface was coated by a black paint for this measurement (it is not needed if thermal imaging is used for delamination detection). The predicted TBC conductivity and heat capacity distributions are shown in Fig. 2. It is seen that the predicted thermal conductivity and heat capacity images are uniform. The predicted average TBC conductivity is 1.65 W/m-K, which is consistent with the typical value of such EBPVD TBCs (1.71 W/m-K)¹² obtained from standard laser flash method. The predicted average TBC heat capacity is 3.3 J/cm³-K, which is higher than typical EBPVD TBCs. The reason for a higher predicted heat capacity is probably due to the black-coat thickness and its penetration inside the columnar structure of the EBPVD TBC. Nevertheless, these results indicate that the multilayer modeling method can be used to predict TBC conductivity.

To verify the prediction accuracy, Fig. 3 compares the experimentally measured data and the corresponding theoretical data for a typical pixel within the image. Although the data fit was carried out for the temperature (Fig. 3a), the fitting was also found to be very accurate for the temperature derivative, Fig. 3b.

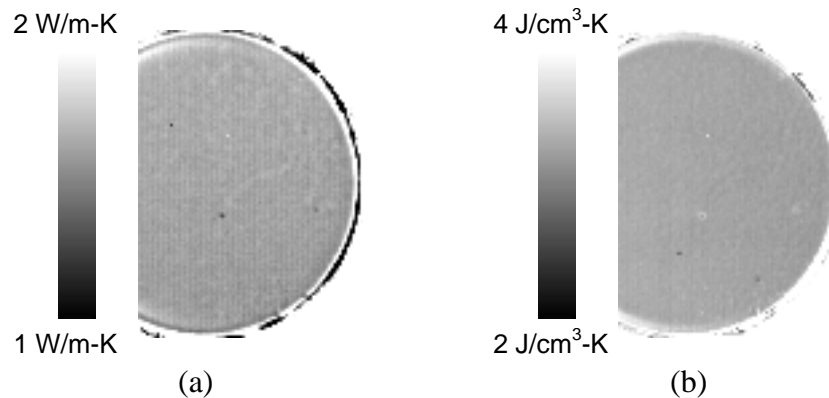


Fig. 2. Predicted TBC (a) conductivity and (b) heat capacity images of a TBC specimen.

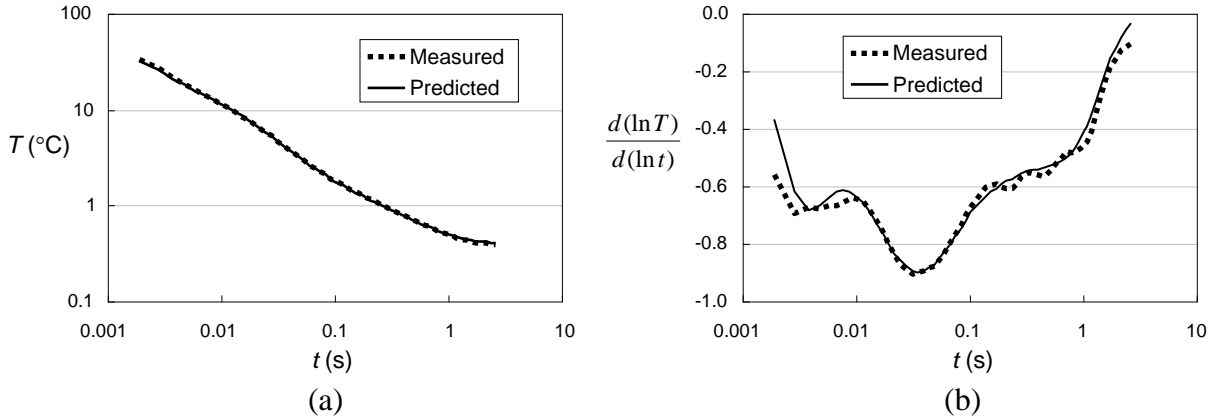


Fig. 3. Comparison of measured and predicted surface (a) temperature and (b) temperature-derivative data for a typical pixel in the Fig. 2 images.

TBC Degradation Monitoring Based on TBC Thermal Properties

A few NDE methods have been proposed to monitor TBC degradation condition, including the Mid-IR reflectance¹³ and impedance spectroscopy¹⁴. These methods are generally based on the relative change of a physical parameter from its initial condition, so they are not quantitative and difficult to use in practical applications.

Because the multilayer modeling method can measure TBC thermal conductivity, which is an intrinsic TBC property, it may be used to monitor TBC degradation condition and predict TBC life. The change of TBC conductivity with thermal exposure has been studied by many authors¹⁵⁻¹⁶. In early exposure times, TBC undergoes a sintering process, resulting in a denser material and an increased conductivity. As exposure time increases, microcracking starts to initiate and extend within the coating and near the interface, so TBC conductivity decreases. When delamination occurs in the later period of the TBC life, a significant conductivity decrease can be observed in the delaminated regions. This characteristic change in TBC conductivity with exposure time can be used to monitor TBC degradation condition and predict TBC life, as long as TBC conductivity distribution can be accurately measured.

This TBC degradation monitoring scheme is illustrated in Fig. 4, which displays measured thermal conductivity images and average values of four EBPVD TBC samples exposed in thermal cycling tests at various durations that are represented by percentage of TBC life (sample courtesy of Mr. A. Luz, Imperial College London). The 100% TBC life is defined as when the total area of TBC spallation exceeds 20% of the surface area. As shown in Fig. 4, the as-processed TBC conductivity was generally uniform at 1.8 W/m-K. At 33% life, TBC conductivity was still uniform, but at a higher value due to sintering. At 67% life, while the majority of the TBC surface had uniform conductivity, many small regions showed reduction of conductivity. The conductivities of two noticeable low-conductivity spots (black spots) are plotted in the figure. These low-conductivity spots should correspond to the locations with microcracking. At 100% life, although TBC spallation occurred in a considerable area (the gray-color region), larger areas of TBC still remained. The conductivity in the remaining TBC area showed either a high value, comparable to the normal values at 33% and 67% TBC life, or a very low value (below the low conductivity bound of 0.8 W/m-K). These low conductivity regions were almost all located at the edges of the remaining TBC, and they had been confirmed to be delamination at the interface¹⁷. These results clearly demonstrate that the average TBC

conductivity, measured by the thermal modeling NDE method, could be a reliable parameter to monitor TBC degradation and predict TBC life.

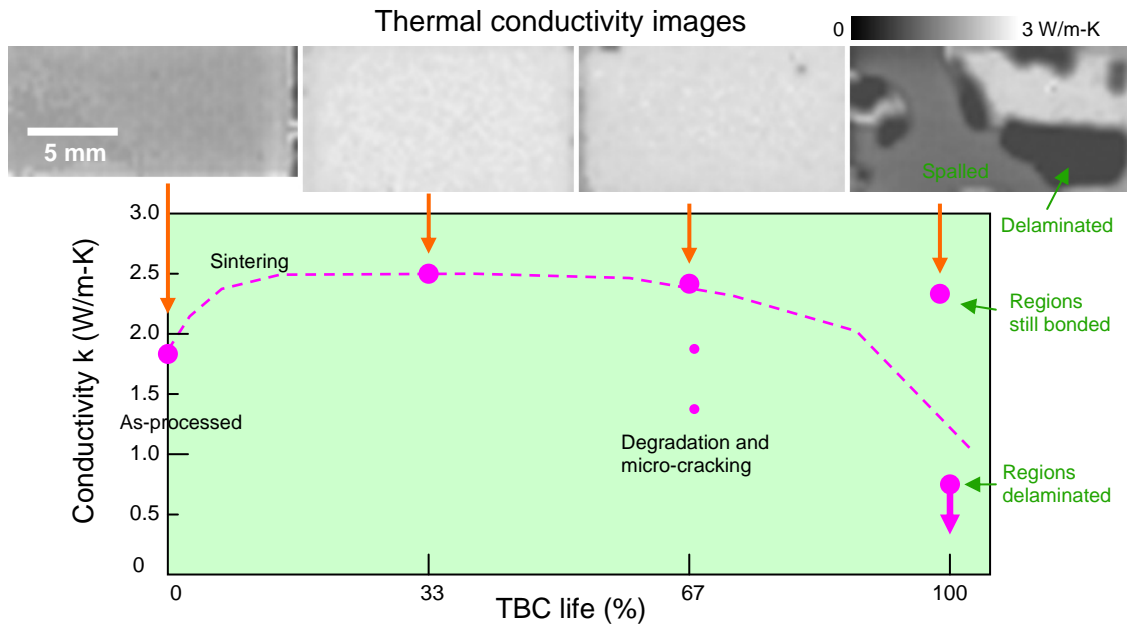


Fig. 4. Measured thermal conductivity of EBPVD TBC samples as function of TBC life.

SYNCHROTRON X-RAY MICRO-CT FOR CERAMIC MEMBRANES

High-temperature ceramic gas-separation membranes were characterized using the microCT system developed at APS beamline 2-BM¹⁸. Figure 5 shows a photograph of the experimental system setup. The synchrotron X-ray source is delivered through a Double Multilayer Monochromator that covers energies between 5 and 30 keV (energy used for testing membranes was at 24 keV). Using a standard detector, a 2048x2048 pixel CoolSnapK4 CCD camera coupled with a CdWO₄ scintillator screen, this corresponds to exposure time between 80 and 200 ms per projection. In this configuration projections are collected at every 1/8 degree (total 180 degree). Including the readout time and disk I/O, data acquisition for a sample takes ~25 minutes. The construction of CT slices is carried out by a cluster computer system. Typical time used to construct all CT slices for a membrane sample was <20 min.

In microCT experiment, each sample was placed on a special mount. Figure 6 shows a photograph of three mounted membrane samples. The spatial resolution is related to the detector pixel size, which is determined by the objective lens of the imaging camera. With a 5X objective, detector pixel size is 1.48 μm. The final result of a microCT experiment is a set of constructed CT slices for a 3D volume of the membrane sample. The data are usually displayed in 2D images, although 3D visualization can also be made.

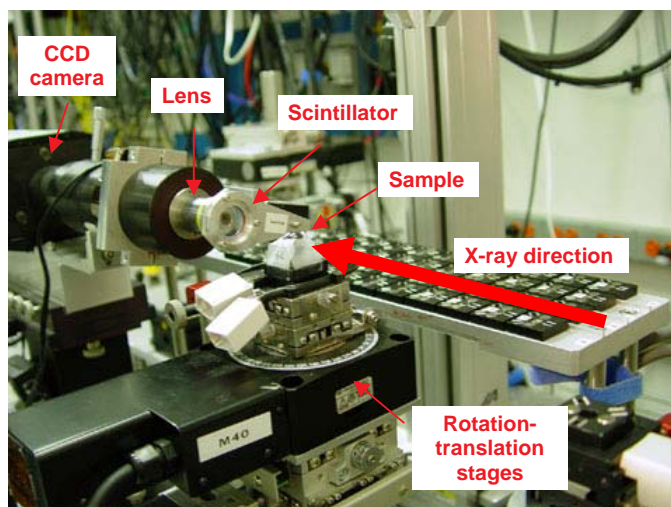


Fig. 5. MicroCT experimental system at APS synchrotron beamline 2-BM.

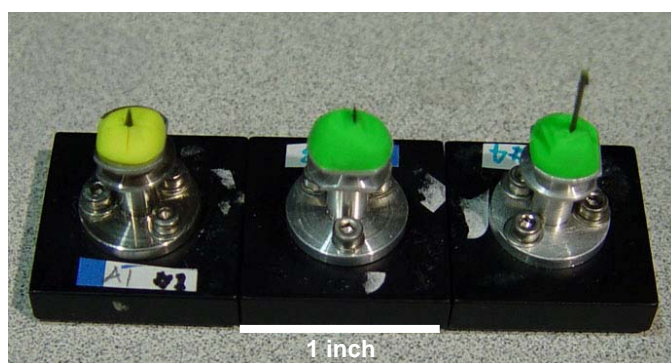


Fig. 6. Mounted membrane samples for microCT test.

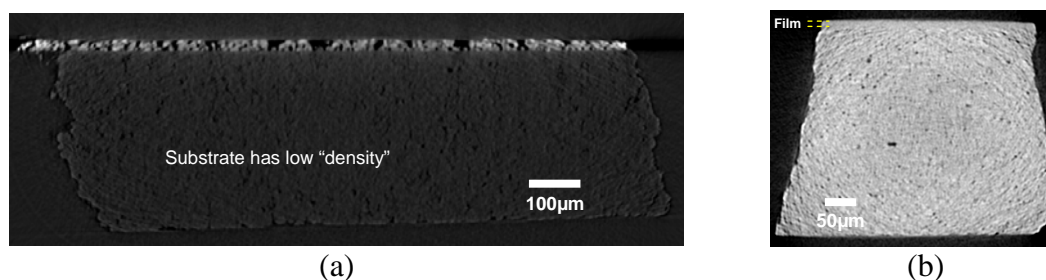


Fig. 7. MicroCT images of membrane samples: (a) Pd/CeO₂ film on Al₂O₃ substrate and (b) BaCe_{0.8}Y_{0.2}O₃ (BCY) film on BCY/NiO substrate.

Figure 7 shows typical microCT slice images of two ceramic membrane samples: Pd/CeO₂ film on Al₂O₃ substrate and BaCe_{0.8}Y_{0.2}O₃ (BCY) film on BCY/NiO substrate (sample courtesy of Dr. T. Lee). For the first sample, Pd/CeO₂ film on Al₂O₃ substrate, it is seen that both the film and the substrate are porous, and the substrate has very low x-ray attenuation coefficient (or low “density”). The microCT images can be used to determine the film thickness (22µm and 10µm for the two samples), porosity distribution, and presence of large pores that could cause leaking. In another experiment, microCT was demonstrated to detect cracks in ceramics with a

crack opening in the order of 0.1 μ m. These results show that microCT may become a valuable NDE technology to characterize ceramic membranes and other functional ceramic materials.

CONCLUSION

Quantitative NDE methods are being developed to determine the physical and geometrical parameters for TBCs and ceramic membranes. For TBCs, a multilayer thermal modeling method was developed to analyze the surface temperature response for TBCs under pulsed thermal imaging condition. Based on a theoretical analysis, it was identified that, among three TBC parameters: thickness L , conductivity k , and heat capacity ρc , only two are independent and can be determined from thermal imaging data. The multilayer-modeling method was used to measure thermal property distributions of an EBPVD TBC sample with known TBC thickness. Measured TBC conductivity was in good agreement with literature value. Based on thermal conductivity data, a new model to monitor TBC degradation was proposed. The model is based on the characteristic change of TBC microstructure (and conductivity) with service time and displayed good experimental correlation for a set of TBC samples exposed at various durations. Therefore, it could become the first practical model to predict TBC life. For gas-separation membranes, x-ray microCT was evaluated to characterize material microstructures and the presence of flaws. It was identified that microCT can determine film thickness, microstructure distribution, and presence of large pores that could cause leaking. These results demonstrated that microCT may become a valuable NDE technology to characterize ceramic membranes and other functional ceramic materials and structures.

ACKNOWLEDGMENT

The author thanks Dr. A. Feuerstein of Praxair Surface Technologies and Mr. A. Luz of Imperial College London for providing TBC specimens and Dr. T. Lee of ANL for providing ceramic membrane samples used in this study, and Drs. F. De Carlo and X. Xiao of ANL for conducting microCT experiments for the membrane samples.

REFERENCES

1. North Atlantic Treaty Organization, "Thermal Barrier Coatings," Advisory Group for Aerospace Research and Development Report, AGARD-R-823, Neuilly-Sur-Seine, France, April 1998.
2. US National Research Council, National Materials Advisory Board, "Coatings for High Temperature Structural Materials," National Academy Press, Washington, DC, 1996.
3. US National Aeronautics and Space Administration, "Thermal Barrier Coating Workshop," NASA Conference Publication 3312, 1995.
4. W.A. Ellingson, S. Naday, R. Visher, R. Lipanovich, L. Gast and C. Deemer, "Development of Nondestructive Evaluation Technology for Ceramic Coatings," Proc. 20th Annual Conference on Fossil Energy Materials, Knoxville, TN, June 12-14, 2006.
5. J.G. Sun, "Method for Analyzing Multi-Layer Materials from One-Sided Pulsed Thermal Imaging," Argonne National Laboratory Invention Report, US patent pending, 2006.
6. J.G. Sun, "Thermal Imaging Characterization of Thermal Barrier Coatings," in *Ceramic Eng. Sci. Proc.*, eds. J. Salem and D. Zhu, Vol.28, no. 3, pp. 53-60, 2007.
7. J.G. Sun, "Method for Thermal Tomography of Thermal Effusivity from Pulsed Thermal Imaging," U.S. Patent No. 7,365,330, issued April 29, 2008.
8. J. G. Sun, "Analysis of Pulsed Thermography Methods for Defect Depth Prediction," *J.*

- Heat Transfer*, Vol. 128, pp. 329-338, 2006.
9. J. G. Sun, "Evaluation of Ceramic Matrix Composites by Thermal Diffusivity Imaging," *Int. J. Appl. Ceram. Technol.*, Vol. 4, pp. 75-87, 2007.
 10. D. L. Balageas, J. C. Krapez, and P. Cielo, "Pulsed Photothermal Modeling of Layered Materials," *J. Appl. Phys.*, Vol. 59, pp. 348-357, 1986.
 11. J.G. Sun, "Thermal Imaging Analysis of Thermal Barrier Coatings," in *Review of Quantitative Nondestructive Evaluation*, eds. D.O. Thompson & D.E. Chimenti, Vol. 28, pp. 495-502, 2008.
 12. A. Feuerstein and A. Bolcavage, "Thermal Conductivity of Plasma and EBPVD Thermal Barrier Coatings," Proc. 3rd Int. Surface Engineering Conf., pp. 291-298, 2004.
 13. J.I. Eldridge, C.M. Spuckler, and R.E. Martin, "Monitoring Delamination Progression in Thermal Barrier Coatings by Mid-Infrared Reflectance Imaging," *Int. J. Appl. Ceram. Technol.*, Vol. 3, pp. 94-104, 2006.
 14. F. Yang and P. Xiao, "Nondestructive evaluation of thermal barrier coatings using impedance spectroscopy," *Int. J. Appl. Ceram. Technol.*, Vol. 6, pp. 381-399, 2009.
 15. H.-J. Ratzler-Scheibe, U. Schultz, "The Effects of Heat Treatment and Gas Atmosphere on the Thermal Conductivity of APS and EB-PVD PYSZ Thermal Barrier Coatings," *Surface & Coating Technol.*, Vol. 201, pp. 7880-7888, 2007.
 16. D. Zhu, S.R. Choi, R.A. Miller, "Development and thermal fatigue testing of ceramic thermal barrier coatings," *Surface & Coatings Technol.*, Vol. 188-189, pp. 146-152, 2004.
 17. J.G. Sun, "Development of Nondestructive Evaluation Method for Thermal Barrier Coatings," Proc. 22nd Annual Conference on Fossil Energy Materials, Pittsburgh, PA, July 8-10, 2008.
 18. F. De Carlo, X. Xiao, and B. Tieman, "X-Ray Tomography System, Automation and Remote Access at Beamline 2-BM of the Advanced Photon Source," Progress in Biomedical Optics and Imaging – Proc. SPIE, Vol. 6318, 2006.